

Obstacle/Gap Detection and Terrain Classification of Walking Robots based on a 2D Laser Range Finder

Patrick Kesper, Eduard Grinke, Frank Hesse, Florentin Wörgötter, and
Poramate Manoonpong*

*Faculty of Physics, Third Institute of Physics - Biophysics
Georg-August-Universität Göttingen,
Friedrich-Hund-Platz 1, 37077 Göttingen, Germany
E-mail: poramate@physik3.gwdg.de

This paper utilizes a 2D laser range finder (LRF) to determine the behavior of a walking robot. The LRF provides information for 1) obstacle/gap detection as well as 2) terrain classification. The obstacle/gap detection is based on an edge detection with increased robustness and accuracy due to customized pre and post processing. Its output is used to drive obstacle/gap avoidance behavior or climbing behavior, depending on the height of obstacles or the depth of gaps. The terrain classification employs terrain roughness to select a proper gait with respect to the current terrain. As a result, the combination of these methods enables the robot to decide if obstacles and gaps can be climbed up/down or have to be avoided while at the same time a terrain specific gait can be chosen.

Keywords: Legged locomotion, Autonomous robots, Climbing, Gap avoidance

1. Introduction

The evaluation of environmental information is the basis to enable autonomous (walking) robots to successfully navigate through complex environments. To tackle this problem different approaches have been proposed. For example, Labecki et al.¹ used a laser range finder (LRF) to build a height map of the environment. Maier et al.² combined monocular vision and LRF readings for humanoid robot navigation. Wooden et al.³ utilized a LRF and stereo vision in combination with complex navigation and perception algorithms. In contrast to these works, here we use a LRF based simple control algorithm without further sensor modalities for obstacle/gap detection and terrain classification. In this paper we will show that such a simple control algorithm is sufficient to enable a hexapod robot to successfully traverse difficult terrains. Furthermore this algorithm can serve as a basis for more complex control structures.

2. Materials and Methods

2.1. The Hexapod Robot AMOSII

AMOS II is a six-legged walking robot⁴ (see Fig. 1) used throughout this work. At the front of the robot, a Hokuyo URG-04LX-UG01 laser range finder (LRF) is mounted on a small tower-like mounting device (Fig. 1). We selected this LRF since it is lightweight, independent from light conditions and needs only little power.⁵ The LRF is mounted at a height of $h = 22.5$ cm, its horizontal angle β is set to 25° (see Fig. 1) for the work at hand. We found this to be the optimal trade off between decreasing look ahead distances for higher angles and reduced accuracy and robustness for lower angles.⁵ Besides the LRF, two ultrasonic sensors are attached at the front part of the robot. These sensors are used for climbing behavior⁴ which is triggered by the presented obstacle/gap detection algorithm (described below).

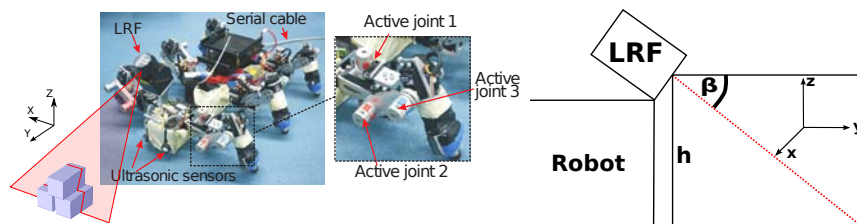


Fig. 1. Left: The walking robot AMOS II with the LRF (overall picture and zoom of leg with three active joints). An illustration of the LRF function is depicted. Right: Sketch of the LRF setup.

2.2. Obstacle/Gap Detection

In the work at hand, we propose an obstacle/gap detection algorithm consisting of three steps. First the raw laser scan data is preprocessed to remove measurement artifacts, then edges of objects are detected based on height differences (see Fig. 1, Left) and in the postprocessing edges are combined to objects. The details of each step are provided in the following subsections.

Preprocessing: In a first step the LRF readings are transformed from spherical into cartesian coordinates. Then, in order to increase robustness of the edge detection, outliers and measurement artifacts such as mixed pixels⁵ are removed. A simple exclusion algorithm based on the deviations

of x and z coordinates (see Fig. 1, Right) between neighboring points is used (see Algorithm 2.1, Left).

Edge Detection Algorithm: In this work, we use a fixed value thresholding algorithm for edge detection.⁶ This algorithm is based on the fact that obstacles/gaps correspond to height differences in the x-z plane of the 2D laser data.⁶ By applying a threshold to the height difference between two data points, edges can be detected.

Postprocessing: Here, neighboring edges with a similar mean height are joined as they have high probability to correspond to only one entity, e.g., a rough object. For the remaining edges average (z_{avg}), maximum (z_{max}) and minimum (z_{min}) values are calculated and compared with thresholds defining obstacles and gaps (see Sec. 2.4).

This algorithm can be applied to detect different types of obstacles including walls and objects having sufficient height different to the ground. It has been successfully tested to detect, e.g., different box sizes.

2.3. Terrain Classification based on Roughness Estimation

Obtaining an estimation of the surface roughness enables walking robots to select a terrain specific gait, thereby performing effective locomotion. We introduce a criterion for roughness estimation based on the amplitude and the rate of height changes of the LRF data. These features are represented in the root-mean-square value $R_q = \sqrt{\frac{1}{n} \sum_{i=1}^n d_i^2}$. It evaluates the deviation d_i of each data point from the average height of the calculated edges. The roughness estimation value can be used to select a gait depending on terrain surface roughness. However, to enhance the robustness of the gait selection, R_q is filtered with a low pass filter.

2.4. Behavior Control for Complex Environments

The processed LRF data provides obstacle/gap and roughness information about the environment used to decide which action the robot should perform. The behavior control based on these data is summarized in Algorithm 2.1, Right. First the minimum and maximum height values are evaluated to detect non crossable objects/gaps. In case of the average height being between the positive and negative ground threshold, no climbing is initiated since this situation is considered as obstacle/gap free. Thus, the robot continues walking forward. On the other hand, if the average height

Algorithm 2.1 Left: Pseudo code for preprocessing LRF data. Right: Pseudo code of behavior control.

<pre> for all p_i in <i>dataPoints</i> do <i>transform</i>(p_i) $\Delta x = p_i.x - p_{i+1}.x$ $\Delta z = p_i.z - p_{i+1}.z$ if $\Delta x > minX$ AND $\Delta z < maxZ$ then <i>save</i>(p_i) else <i>remove</i>(p_i) end if end for </pre>	<pre> if $z_{min} < minHeight$ then <i>turn</i>() else if $z_{max} > maxHeight$ then <i>startObstacleAvoidance</i>() else if $z_{avg} > ground$ then if $dist < distThreshold$ then <i>startClimbing</i>() else <i>startWalkingForward</i>() end if end if if $z_{avg} < -ground$ then <i>startClimbing</i>() else <i>startWalkingForward</i>() end if end if end if </pre>
---	--

is above the positive ground threshold (i.e., climbable obstacle) or below the negative ground threshold (i.e., climbable lower step), climbing behavior is activated. During climbing behavior the front part of the robot is tilted upwards/downwards. These motions are controlled by the ultrasonic sensors-driven backbone joint (see Goldschmidt et al.⁴ for more details). While climbing, the LRF does not produce reliable measurements and thus its values are not used. During locomotion the gait can additionally be changed according to the roughness R_q of the terrain.

3. Experimental Results

3.1. Behavior Control based on Obstacle/Gap Detection

The behavior control using LRF-based obstacle/gap detection was investigated on a track consisting of a ground floor and two elevated platforms. The robot started walking towards the first platform (stage 1, Fig. 2). It continued walking until it was near enough to the platform. It then detected the platform as a climbable obstacle since the average height (z_{avg} , Fig. 2) was above a positive ground threshold. The decreasing distance to the platform can be seen in the increasing outputs of the ultrasonic sensors

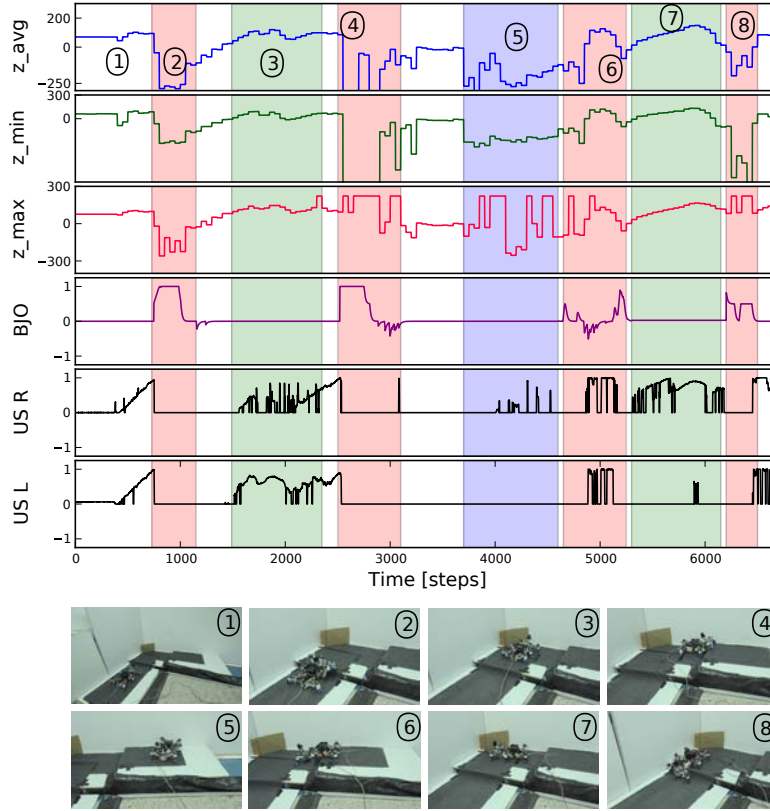


Fig. 2. From top to bottom: Average height of the LRF data (z_{avg}), minimum height in LRF data (z_{min}), maximum height in LRF data (z_{max}), backbone joint signal (BJO) and left and right ultrasonic sensors (US_L , US_R). All height values are given in mm. If the backbone joint signal is positive, the joint is tilted upwards and downwards for negative values. The ultrasonic signals represent the distance to an obstacle, where a higher value is obtained for nearer obstacles (zero represents no obstacle in field of view). Within the green areas the robot avoided obstacles, while in the blue area a gap was avoided by turning. Within the red areas, the climbing routine was enabled. In these areas the output of the LRF was ignored.

(US_L , US_R , Fig. 2). As these values exceeded a threshold, the robot started to climb (stage 2). The progress of the climbing routine is represented by the backbone joint motion. At the beginning the front part of AMOS II moved up to reach the edge of the obstacle, indicated by an increase in the backbone joint signal (BJO, Fig. 2). Afterwards the front part bent down to support the climbing of the main body, hence the backbone joint signal decreased to negative values until the climbing finished. While walking on

the first platform the robot detected the wall in front of it. The height of the wall was correctly classified as too high to climb (z_{max} , Fig. 2) and the robot then turned (i.e., obstacle avoidance, stage 3). At some point the wall vanished from the field of view, the robot thus made some forward steps until the wall appeared again in its field of view. This can be seen in the ultrasonic sensor outputs oscillating around the distance threshold value. After avoiding the wall, the robot climbed onto the second platform (stage 4), showing a behavior similar to the first climbing procedure. On top of the second platform only the LRF was able to detect the gap limiting the platform. Its minimum value z_{min} decreased below the gap threshold. The robot turned until facing the first platform again (stage 5). At this point the robot climbed down, as the average height z_{avg} was between gap and ground thresholds. Again the climbing routine can be recognized by the backbone joint signal (stage 6). After climbing down to the first platform the robot walked forwards, avoided the wall directly in front (stage 7) and then climbed down to the ground (stage 8).

This experiment shows that the behavior control based on LRF data proposed in Sec. 2.4 allows the robot to autonomously locomote on the complex terrain. We recommend readers to also see the supplementary video of this experiment at <http://manoonpong.com/CLAWAR2013/suppl.wmv>.

3.2. Behavior Control based on Terrain Classification

To evaluate the terrain classification using LRF data as described in Sec. 2.3, an experimental track was built, where the robot has to traverse three areas with significant differences in roughness. The starting point was on a flat wooden platform (area 1). From there the robot had to continue to walk over fine (area 2) and coarse-grained gravel (area 3). The gait of AMOS II can be controlled via one control input.⁴ In this experiment this input was determined by the result of the terrain classification (R_q). Figure 3 shows the sensor data of the robot while traversing the different terrains. As expected R_q was very small on the wooden platform (area 1), thus a fast walking pattern was chosen (tripod gait).

When arriving at the second area the filtered R_q increased to values between 5 and 25. This resulted in a gait change, from a tripod gait to a wave gait, which is slower and better suited for fine gravel.

In front of the third area the filtered R_q value increased above 25. This led to a change of the wave gait to a tetrapod gait, which enabled the robot to perform faster and proper walking on uneven terrain, like the coarse-grained gravel. The successful completion of this track indi-

icates that the terrain classification provided by the LRF can be used to choose gaits according to the terrain the robot approaches. We recommend readers to also see the supplementary video of this experiment at <http://manoonpong.com/CLAWAR2013/suppl.wmv>.

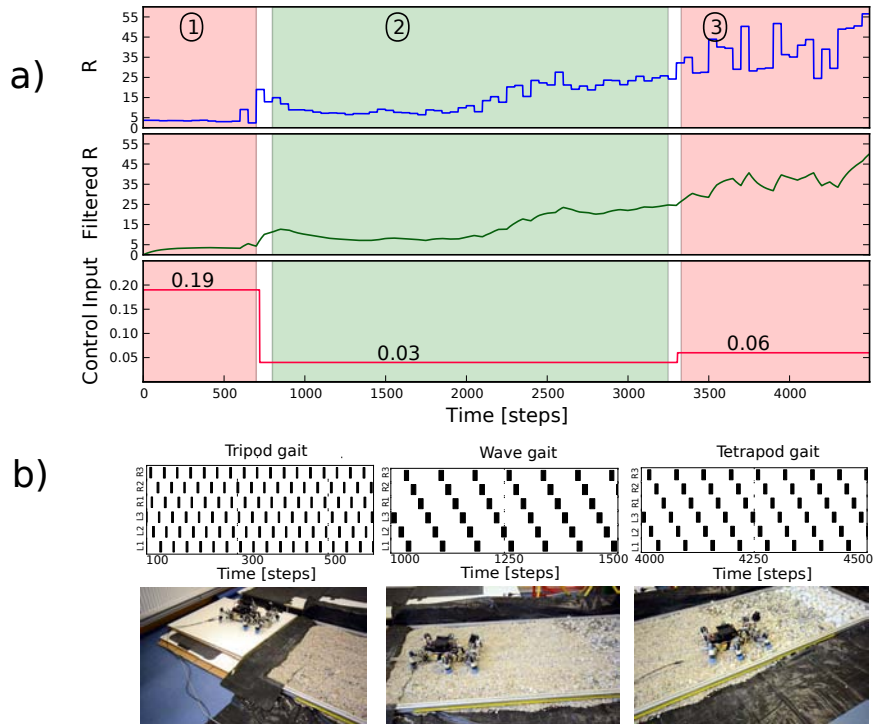


Fig. 3. Signals and pictures of the robot while traversing different terrains. a) The first two rows show the raw and filtered results of the terrain classification (R_q) followed by the control input which determines the gait of the robot. b) The gaits used by AMOS II shown as gait diagrams (black swing phase, white stance phase) and below the places in the track where these gaits are used.

4. Conclusion

We showed that a 2D LRF can be used for obstacle/gap detection. This allows the hexapod robot to climb up and down platforms surrounded by walls and deep gaps. Furthermore, terrain classification based on LRF data can be used to adapt the gait of the robot to different terrains, like flat ground and different grained gravels.

However there are still some aspects which can be improved. Basically, the LRF can provide position and width information about obstacles in its field of view. This information could be used to determine the direction of turning when facing several obstacles with different heights or provide a basis for more advanced behavior control. With this enhancement the robot will be able to navigate in more complex environments than the comparatively simple setup used in this paper. In particular the robot would be able to judge if it would be better, e.g. in terms of energy or danger, to climb or to avoid an obstacle instead of using a decision based on the maximal climbable heights only. Furthermore the algorithm can be extended to measure the length of objects by using memory and simple navigation techniques. In addition, the thresholds for terrain classification and the corresponding gaits were set by hand. In real world applications, where the terrain is usually not known, a more elaborate threshold and gait selection can be necessary. This could possibly be achieved by learning techniques.^{7,8}

Acknowledgments: This research was supported by Emmy Noether grant MA4464/3-1 of the Deutsche Forschungsgemeinschaft, the Bernstein Center for Computational Neuroscience II Göttingen (BCCN grant 01GQ1005A, project D1) and the Bernstein Focus Neurotechnology Göttingen (project 3B, 01GQ0811).

References

1. P. Labecki, D. Rosinski and P. Skrzypczynski, *Transactions of the ASME, Journal of Basic Engineering* (2011).
2. D. Maier, M. Bennowitz and C. Stachniss, Self-supervised obstacle detection for humanoid navigation using monocular vision and sparse laser data, in *Proc. IEEE Int. on Robotics and Automation (ICRA)*, 2011.
3. D. Wooden, M. Malchano, K. Blankespoor, A. Howardy, A. Rizzi and M. Raibert, Autonomous navigation for bigdog, in *Proc. IEEE Int. on Robotics and Automation (ICRA)*, 2010.
4. D. Goldschmidt, F. Hesse, F. Wörgötter and P. Manoonpong, Biologically inspired reactive climbing behavior of hexapod robots, in *Proc. IEEE Int. Conf. on Intelligent Robots and Systems (IROS2012)*, 2012.
5. Y. Okubo, C. Ye and J. Borenstein, Characterization of the Hokuyo URG-04LX laser rangefinder for mobile robot obstacle negotiation, in *Proc. SPIE*, 2009.
6. G. A. Borges and M.-J. Aldon, *J. Intell. Robot. Syst.* **40**, 267 (2004).
7. S. Steingrube, M. Timme, F. Wörgötter and P. Manoonpong, *Nature Physics* (2010).
8. P. Manoonpong, C. Kolodziejski, F. Wörgötter and J. Morimoto, *Advances in Complex Systems* (2013).